Indian Journal of Pure & Applied Physics
Vol. 55, May 2017, pp. 339-344

An experimental study of energy dependence of saturation thickness of multiply scattered gamma rays in zinc

Gurvinderjit Singh[a], B S Sandhu[b] & Bhajan Singh[b]*

[a]Government Girls Senior Secondary School, Bharat Nagar, Ludhiana 141 001, India
[b]Physics Department, Punjabi University, Patiala 147 002, India

Received 20 February 2016; revised 23 February 2017; accepted 14 March 2017

The present measurements have been carried out to study the energy dependence of saturation thickness of multiply scattered gamma photons from zinc targets of various thicknesses. An inverse response matrix approach has been implemented to convert the observed pulse-height distribution of a NaI (Tl) scintillation detector to a photon spectrum and hence to improve the statistical error. These results in extractions of intensity distribution of multiply scattered events originating from interactions of 662 keV photon with thick target of zinc material. The observed pulse-height distributions are a composite of singly and multiply scattered events. To evaluate the contribution of multiply scattered events only, the spectrum of singly scattered events contributing to inelastic Compton peak has been reconstructed analytically. The scattered photons have been detected by a properly shielded NaI (Tl) gamma ray detector placed at different angle to the incident beam. The saturation thickness at which the number of multiply scattered events saturates has been measured. The signal-to-noise ratio and multiple scatter fractions have been found to be decreasing with increasing target thickness. The self-absorption correction factor improves the multiply scattered photon intensity but not the saturation thickness. The same experiment has been repeated with HPGe detector at 90° scattering angle. The results obtained with NaI (Tl) and HPGe detector show the same trend. The experimental results have been found to support the Monte Carlo calculations.

Keywords: Singly and multiply Compton scattered events, Saturation thickness, Signal-to-noise ratio, Monte Carlo methods, Multiple scatter fraction

1 Introduction

Multiple scattering is useful in a variety of fields, like medical diagnostic radiological techniques (CAT scanner, SPECT, PET, DEXA, etc.), non-destructive testing of industrial and agricultural samples to enhance contrast of the image because the samples to be investigated are of finite dimensions. In Compton profile measurements, the interactions of photons with the target material may result in significant fraction of multiply scattered photons in addition to singly scattered ones. The energy spectrum of such photons is broad and never completely separated from the singly scattered distribution in real measurements. This leads to the smearing of information associated with the intensity change of scattered photons. Photons continue to soften in energy as the number of scatterings increases in the sample. So the multiply scattered photons become one of the principle difficulties for interpreting data as these radiations may also reach the detector along with singly scattered ones and the unique relation between photon energy and electron momentum[1,2] is lost. Three different approaches[3] have been used to estimate the contribution arising from multiply Compton scattered radiation[2]. The multiple scattering has been investigated both experimentally and theoretically using analytical and Monte Carlo methods. The analytical approaches[4-7] to study of multiple scattering generally do not provide all the information required to correct the Compton profile data for this contamination because of complicated nature of the scattering processes and different geometrical constraints. Therefore, Monte Carlo methods are commonly used to predict for the contribution of multiple scattering. Monte Carlo studies[7-10] relate multiple scattering to finite sample dimensions. Different scattering geometries have been suggested to minimise the contribution of multiple scattering, but no systematic study of the shape of the energy distribution of multiply scattered radiation under various experimental conditions exists. Our measurements[11] provide a complete survey of analytical and Monte Carlo simulation approaches to study the multiple scattering and available experimental data on these processes. These

*Corresponding author (E-mail: bhajan2k1@yahoo.co.in)

measurements have confirmed that the numbers of multiply scattered events, having same energy as in singly scattered distribution, increase with increase in target thickness and then saturate after a particular thickness of the target known as saturation thickness. The saturation thickness is found to be decreasing with increasing atomic number of the target. These measurements also provide the intensity and energy distributions of 662 keV photons multiply scattered from a zinc target of various thicknesses at a scattering angle of 90° with the scattered photons being detected by an HPGe gamma detector. Paramesh *et al.*[12] have measured Z-dependence of saturation depth of 662 keV multiply scattered gamma rays at 120° for aluminium, iron, copper and lead. Barnea *et al.*[13] have measured the distribution of multiply scattered photons at 662 keV energy for samples of aluminium, brass and tin at 90° and 120°, and compared the experimental results with the Monte Carlo simulations (ACCEPT code in ETRAN model) developed according to the geometry of their experiment. Shengli *et al.*[14] have performed experiment to detect an iron object embedded in the large concrete wall at 662 keV using NaI(Tl) scintillation detector. By simulating their experiments with the Monte Carlo simulation in the EGS4 package, they concluded that the presence of multiple Compton scattering impairs the contrast between the background and the object. Singh *et al.*[15] investigate the effect of detector collimator and the sample thickness on 662 keV multiply Compton scattered photons from cylindrical samples of aluminium, and confirm that in order to increase the signal-to-noise ratio, multiple scattering background should be minimised and can be achieved by using a narrow detector collimation. In the present work, an inverse matrix approach to correct for multiple scattering contributions has been implemented which first converts the observed pulse–height distribution to photon spectrum response function of scintillation detector and then helps low energy pulse-height counts resulting from partial absorption of higher energy photons to be shift under the photo-peak. The events left in the Compton continuum accounts for photons of reduced energy originating from multiple interactions in the target and finally escaping in direction of gamma detector. This procedure enhances the statistical accuracy of the multiple scatter data. The present experiment is performed at 662 keV incident photon energy to achieve this stated objective. In the experimental procedure, the scattered photons are detected from the zinc target in reflection and transmission geometries at various possible scattering angles in the range from 50° to 140°.

2 Experimental Set-Up and Method of Measurement

In the present measurements, a ^{137}Cs radioactive source of strength 222 GBq (~6 Ci) emitting 662 keV gamma rays is used. This radioactive source is in the form of pellets of CsCl sealed in an aluminium can of diameter 27 mm and length 80 mm. The details of experimental set up have been discussed in details elsewhere[11] and the experimental arrangement is shown in Fig. 1.

An intense collimated beam of gamma photons from the radioactive source is allowed to impinge on the target of a given material. The source-target assembly is aligned in such a way that the incident photon beam is confined to the target only. The distance between the fine beam collimator and the front face of the target is kept at 320 mm. An integrated gamma detector assembly is used to detect the scattered photons that consist of 51 mm diameter × 51 mm thick NaI (Tl) scintillation crystal, having 0.38 mm thick aluminium window and optically coupled to RCA-8053 photomultiplier tube. The gamma detector is shielded by cylindrical lead shielding (140 mm in length and 27.5 mm thick) of inner diameter 60 mm. The inner side of this shielding is covered with 2 mm thick iron and 1 mm thick aluminium with iron facing towards lead to absorb the lead K X-rays emitted by lead shielding. The detector is placed on a movable arm, which can rotate around the target mount on the scattering table. The scattered beam is further collimated by a cylindrical collimator (internal radius 2 mm and thickness 17 mm) of lead lined with aluminium, placed at a distance of 25 mm in front of the gamma detector. The principle of

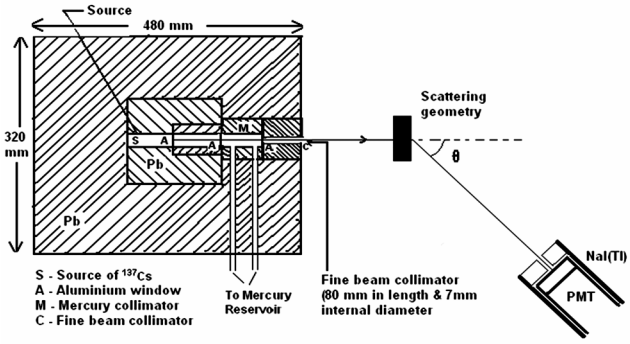

Fig. 1 — Experimental arrangement for present measurements

measurements of multiply scattered photons is based upon the detection of all the scattered photons, originating from interactions of primary gamma photons with the targets of various thicknesses, by placing a properly shielded NaI(Tl) scintillation detector at various scattering angles relative to the incident beam. The observed spectra are a composite of singly and multiply scattered events in addition to events arising from other interaction processes. In order to determine contribution of multiply scattered photons only, the spectrum of singly scattered photons is reconstructed analytically the details of which is discussed by Singh *et al.*[11] The singly scattered spectrum is normalized at full energy peak of the measured pulse-height distribution to obtain the contribution of singly scattered photons under the measured spectrum. This normalized peak intensity distribution is then divided by peak-to-total ratio of the detector corresponding to peak energy, and is subtracted from the observed scattered spectrum to obtain the events originating from multiple scattering. These multiply scattered events when corrected for the photo-peak efficiency of the detector provide the emergent flux from the target having energy in the range of inelastically scattered peak distribution in the direction of the detector.

3 Results and Discussion

A typical observed scattered spectrum (curve-a of Fig. 2), for 10 ks irradiation time, originating from interactions of 662 keV incident photons with the zinc target (3 mm thick) is a composite of singly as well as multiply scattered photons along with background events. The curve-b accounts for recorded events unrelated to the target for the same duration of time. The subtraction of events under the curve-b from those under the curve-a, results in scattered spectrum (curve-c of Fig. 2) which consists of intensity distribution of singly as well as multiply scattered photons. The singly scattered events under the full energy peak are obtained by reconstructing analytically the singly scattered inelastic peak (shown by curve-d in Fig. 2) using the experimentally determined parameters, such as FWHM and detector efficiency of the detector corresponding to the singly scattered energy. The events under curve-d of Fig. 2 are subtracted from the events under the full energy peak of experimental pulse height distributions which results in multiply scattered events only having the same energy as in singly scattered Compton distribution. The above procedure is repeated for different target thickness of the zinc scatterer at different scattering angle varying from 50° to 140°. In Fig. 3 curve-a shows the experimental pulse height distribution of the curve-a of Fig. 2, curve-b is singly scattered photon spectrum reconstructed analytically and curve-c is calculated histogram plotted using inverse response matrix approach for 20 mm thick zinc target with gamma detector placed at 90° to the

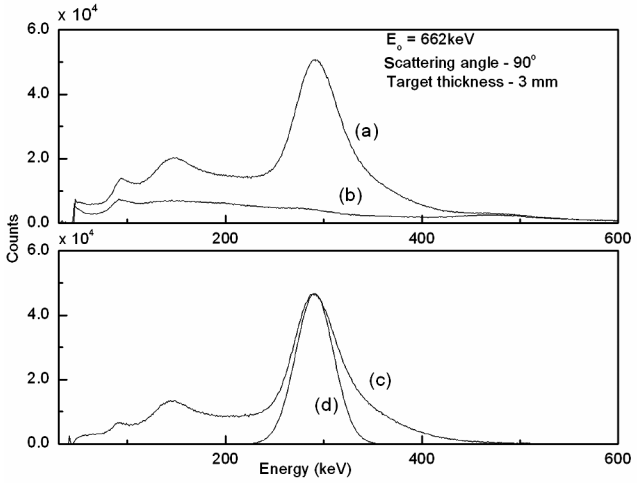

Fig. 2 — (a) A typical experimentally observed spectrum of 662 keV incident photons with zinc target of 3 mm thickness at scattering angle of 90°, (b) observed background spectrum without zinc target in the primary beam, (c) experimentally observed pulse-height distribution, obtained after subtracting background events and (d) normalised analytically reconstructed singly scattered full energy peak

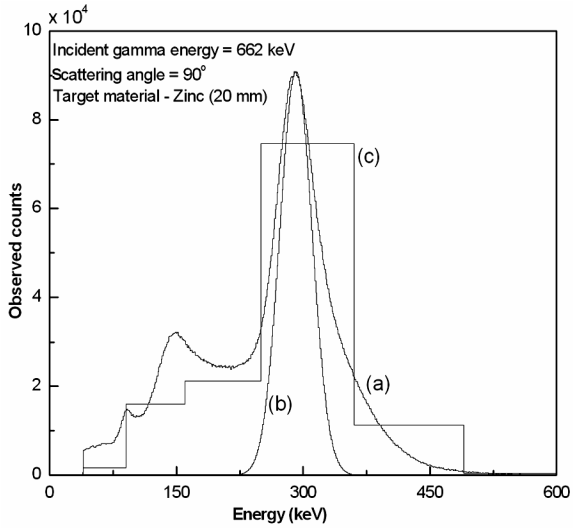

Fig. 3 — (a) A typical experimentally observed spectrum of 662 keV incident photons with zinc target of 20 mm thickness at scattering angle of 90°, (b) normalised analytically reconstructed singly scattered full energy peak and (c) calculated histogram converting pulse-height distribution to a photon spectrum

incident beam. The events under the calculated histogram corresponding to energy range from 220 to 370 keV accounts for singly and multiply scattered radiations having energy equal to that of singly scattered ones. The events under curve-b of Fig. 3 are divided by peak-to-total ratio of the gamma detector and then their subtraction from the events under the calculated histogram (curve-c) in the specified energy range results in events due to multiple scattering having the same energy as in singly Compton scattering. These residual events divided by intrinsic efficiency of NaI(Tl) crystal provide the emergent flux from the zinc scatterer at 90° having energy in the range of inelastically scattered peak distribution. The present experimental results show that the number of multiply scattered events, increases with an increase in the target thickness and saturates after a particular value of target thickness called saturation depth. The saturation of multiply scattered photons is due to the fact that as the thickness of target increases, the number of scattered events also increases but the number of photons coming out of the target decreases. So a stage is reached when the thickness of the target becomes sufficient to compensate the above increase and decrease of the number of photons. The intensity of multiply scattered photons also increases more using detector response function approach as compared with the intensity without the detector response approach, but saturation thickness remains the same as shown in Fig. 4. A small decrease in the intensity of multiply scattered photons at increasing target thickness is due to absorption of incident photons and further attenuation of scattered radiation in the target before reaching the detector. The saturation thickness at low scattering angles less than 90° is determined in the transmission geometry, while the saturation for large scattering angles greater than 90° is determined in the reflection geometry. As the scattering angle increases, the scattered photon energy decreases and hence the saturation thickness changes depend upon the distance travelled by the scattered gamma photons in the target material. So the saturation thickness is energy dependent for a particular target material. The experimental results for zinc target using NaI(Tl) scintillation detector are also compared with experimental results determined by HPGe detector. The saturation thicknesses obtained with these two detectors have the same value. The present experimental results are compared with the data simulated with Monte Carlo package developed by Bauer and Pattison[17]. The theoretical data based upon Monte Carlo calculations for multiply scattered intensity at scattering angle of 50°, 70°, 90° and 140° along with experimental results is shown in Fig. 5. The simulated data of multiply scattered intensity supports the present experimental results. The deviation of some of the simulated data points from experimental values is caused by non-inclusion of

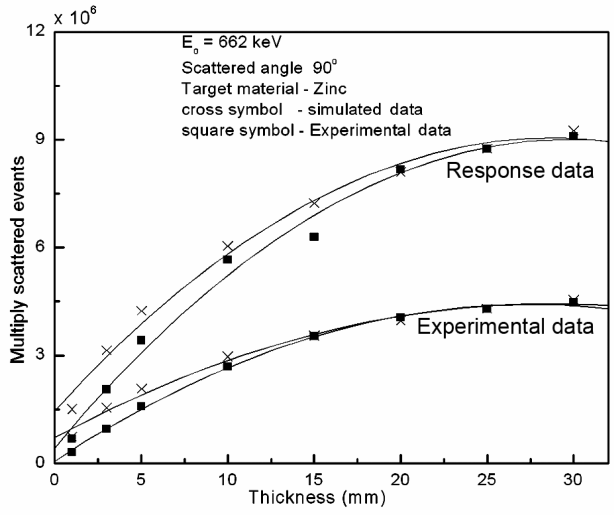

Fig. 4 — Variation of observed number of multiply scattered events as function of thickness of the zinc target for 662 keV photon energy at scattering angle 90° (■) and simulated data by Monte Carlo method (×)

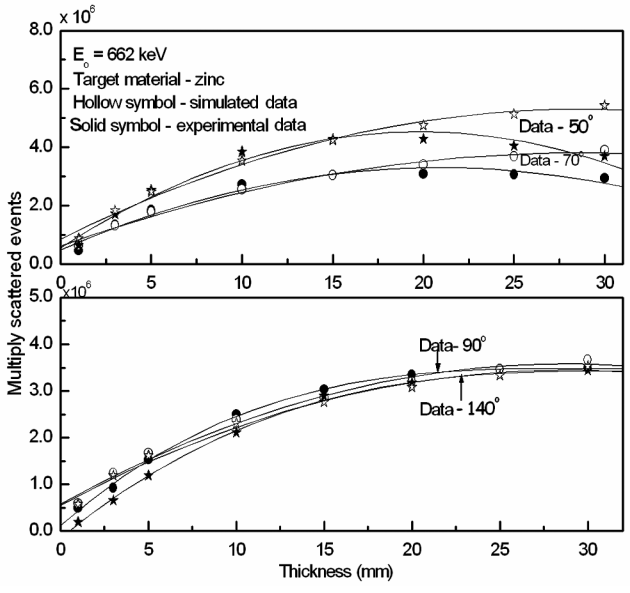

Fig. 5 — Variation of observed number of multiply scattered events as function of thickness of the zinc target for 662 keV photon energy at scattering angles of 50°, 70°, 90° and 140° (solid symbol) and simulated data by Monte Carlo method (hollow symbol)

scattering contributions from moving electrons and polarization effects of scattered photons, which are not included in the present Monte Carlo package.

As the thickness of the target increases the wings of the Compton scattered peak are broadened due to multiple scattering which concentrates approximately at the lower half of the scattered peak. The top half of the peak has a negligible amount of multiple scattering and is determined by a factor called the multiply scatter fraction (MSF). This factor contributes a background which reduces the quality of the image in Compton scatter imaging for non-destructive testing of samples[13], and is expressed as:

$$MSF = \frac{Ms}{M_m + M_s} \quad \ldots (1)$$

where M_m and M_s are the numbers of multiply and singly scattered photons under the Compton scattered peak, respectively. In the present study, zinc target of thickness of 1 mm, 10 mm and 30 mm considered to have significant amount of multiple scattering at 662 keV incident photon energy is chosen for the determination of M_s. The area under this Compton scattered peak with the target is subtracted from the area under the experimentally measured Compton scattered peak with thick targets to obtain the amount of multiply scattered photons only. For this purpose, the exact position of the centroid of the scattered peak is required and is calculated with the help of Compton scattered energy formula for a given energy. An energy window of about 20 keV is chosen across this centroid and area under this energy window is determined. Next, the width of energy window is increased by 20 keV and the area under the peak is noted. This procedure, of increasing window width by 20 keV, is repeated and the MSF value for each window is determined. Figure 6 shows that the MSF decreases slowly for low energy window for 1 mm thickness than 10 mm and 30 mm thick target which means that multiple scattering is more in thick target than thin target. Figure 7 compares the MSF at scattering angles of 60°, 90° and 120° for zinc target of thickness 1 mm and 30 mm. It is clear that as the thickness of the target increases, MSF also increases. Also the contribution of multiple scattering increases more in the low energy side of the Compton scattered peak as compared to the high energy side of spectrum which is due to dominance of Compton - Compton scattering process as compared to the Rayleigh-Compton and Compton-Rayleigh processes. In Compton profiles and cross-section measurements, only the singly scattered photons entering the detector are desired and the multiply scattered photons act as background noise which is to be minimized by this procedure.

The signal-to-noise ratio (ratio of number of singly scattered events to number of multiply scattered

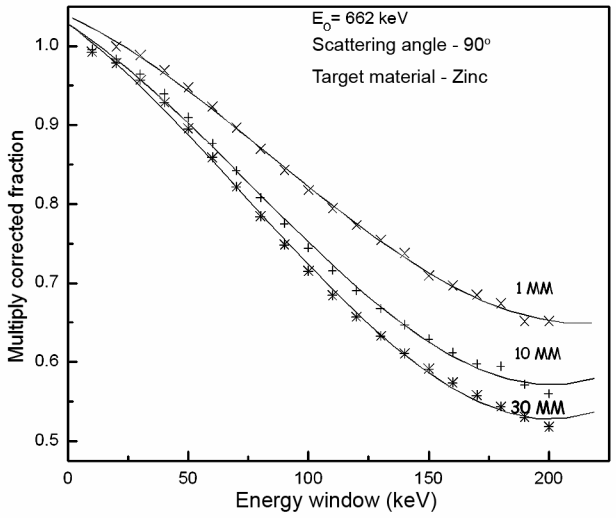

Fig. 6 — Plot of multiply scattered fractions (MSF) as function of energy window around the Compton scattered peak centroid for 662 keV photon energies for different thickness at scattering angle 90°

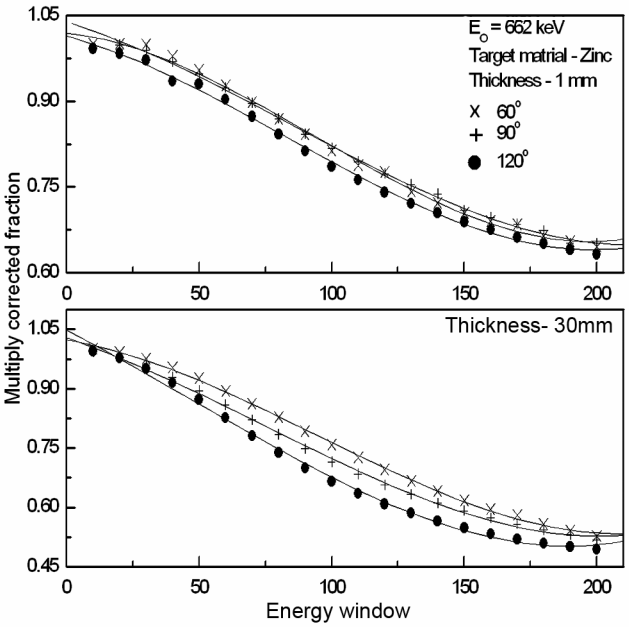

Fig. 7 — Plot of multiply scattered fractions (MSF) as function of energy window around the Compton scattered peak centroid for 662 keV photon energy at scattering angles of 60°, 90° and 120° for target thickness of 1 mm and 30 mm

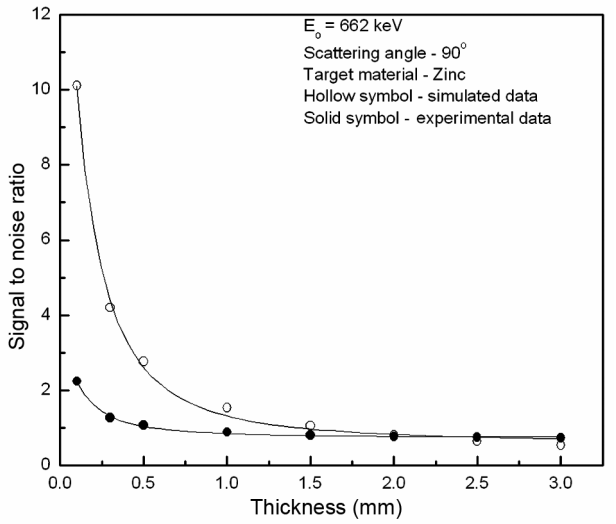

Fig. 8 — Variation of signal-to-noise ratio as function of target thickness for 662 keV photons at scattering angle of 90° (Solid symbol) and simulated data (hollow symbol)

events) is plotted as a function of target thickness for 662 keV incident photons in Fig. 8. It is clear that when the target thickness increases, the signal-to-noise ratio decreases, indicating the presence of more multiply scattered events in comparison to the singly scattered events. A similar order to increase the signal-to-noise ratio, multiple scattering background should be minimised which can be achieved using thin targets.

4 Conclusions

The experimental results of this study confirm that for thick targets, there is significant contribution of multiply scattered radiation emerging from the target, having energy equal to that of singly scattered Compton process. The saturation of intensity of multiple scattering events beyond a particular thickness supports the work of Paramesh *et al.*[12] The saturation thickness increases with increase in incident photon energy. The saturation of multiply scattered fraction (MSF) above a particular energy window around the centroid of inelastic scattered peak supports the work of Barnea *et al.*[13] The signal-to-noise ratio decreases with an increase in target thickness. The detector response function unfolding converts the observed pulse-height distributions to a photon energy spectrum is quite satisfactory. The response function technique improves the multiply scattered photon intensity and hence the statistical accuracy, but not the saturation thickness. In comparison to above measurements, no doubt the use of an HPGe detector provides more faithful reproduction of the shape of distribution of the photons originating from the interactions of incident photons with the target but the saturation thickness remains the same. The simulated data supports the experimental results of present study and shows the similar behaviour.

References

1 Klein O & Nishina Y, *Z Physik,* 52 (1929) 853.
2 Cooper M J, *Rep Prog Phys*, 48 (1985) 415.
3 Copper M J, Mijnarends P E, Shiotani N, Sakai N & Bansil A, *X-ray Compton scattering*, (Oxford University Press, Oxford), 2004.
4 Dumond J W M, *Phys Rev*, 36 (1930) 1685.
5 Williams B G, Pattison P & Cooper M J, *Phil Mag*, 30 (1974) 307.
6 McIntire W R, *Phys Stat Sol*, 23 (1974) 359.
7 Tanner A C & Epstein I R, *Phys Rev*, 13 (1976) 335.
8 Halonen V, Williams B G & Paakkari T, *Physica Fennica*, 10 (1975) 107.
9 Williams B G & Halonen V, *Physica Fennica*, 10 (1975) 5.
10 Felsteiner J, Pattison P & Cooper M J, *Phil Mag*, 30 (1974) 537.
11 Singh M, Singh G, Sandhu B S & Singh B, *Phys Rev*, 74 (2006) 373.
12 Paramesh L, Venkataramaih P, Gopala K & Sanjeevaiah H, *Nucl Instr Meth*, 206 (1983) 327.
13 Barnea G, Dick C E, Ginzburg A, Navon E & Seltzer S M, *NDT E Int*, 28 (1995) 155.
14 Shengli N, Jun Z & Liuxing H, *Proceedings of the Second International Workshop on EGS* (KEK proceedings 200-20, Tsukuba, Japan, 2000), 216.
15 Singh M, Singh G, Sandhu B S & Singh B, *Appl Radiat Isot*, 64 (2006) 373.
16 Sharma A, Singh K, Singh B & Sandhu B S, *Nucl Instr Meth B*, 269 (2011) 247.
17 Bauer G E W & Pattison P, *Compton scattering experiments at HMI*, HMI-B364, (1981) 1.